Multimodal Nanodiamond Drug Delivery Carriers for Selective Targeting, Imaging, and Enhanced Chemotherapeutic Efficacy

*Xue-Qing Zhang, Robert Lam, Xiaoyang Xu, Edward K. Chow, Ho-Joong Kim, and Dean Ho**

Major goals within the development of nanomedicine for cancer therapy include enhancing therapeutic efficacy, the selective targeting of cancerous cells and the ability to track drug import.[1] The advancement of next-generation nanocarriers as drug delivery platforms will require the incorporation of these useful properties, through which adverse side effects of chemotherapy drugs can be avoided and overall treatment and diagnosis improved. As such, a variety of nanoparticle-based delivery systems have already been widely investigated and provided interesting avenues of research for improving cancer treatments through therapy and targeted delivery.[2–7]

Herein, we report on an inclusive multicomponent nanodiamond (ND)-based drug delivery system with simultaneous capabilities in targeting, imaging and enhanced therapy. NDs, 2–8 nm diameter carbon carriers of truncated octahedral composition, have been emerged as promising drug carriers due to their unique features, including biocompatibility,[8–10] functionalization versatility[11] and unique surface electrostatics.[12] In particular, the utilization of NDs has circumvented many individual challenges in cancer therapy, including bypassing chemoresistance,[13] controlled delivery[9] and intracellular tracking.[14–16] A broad range of therapeutics, such as small molecule drugs and nucleic acids have been bound to the ND surface and efficiently delivered with increased efficacy.[9,17] Recent in vivo studies have also alluded to the clinical potential of utilizing ND to deliver chemotherapeutic agents.[13] Fluorophore conjugation and introduction of nitrogen defects have also provided a means of tracking NDs within biological samples.[15,18,19] Thus far, the development of multifunctional NDs as drug delivery platforms with simultaneous capabilities in targeting, imaging and therapeutic activity has yet to be reported. For this, we have synthesized a versatile ND construct that incorporates a targeting agent, imaging agent and chemotherapeutic for multimodal imaging and therapeutic applications. The enhanced therapeutic efficacy and specific internalization within cancerous cell lines is then observed and evaluated.

Active targeting of drugs in a disease specific manner is an appealing approach towards the treatment of cancers.[1] In particular, an effective strategy in treating cancer involves the specific targeting of antigens within tumors of interest.[20] Through ligand-target biorecognition of tumor cells, the toxicity to healthy surrounding cells can be minimized. The receptor tyrosine kinase, human epidermal growth factor receptor (EGFR), is a potent and well studied target for anticancer drug delivery systems. EGFR is overexpressed in over one-third of all solid tumors, including breast, lung, colorectal and brain cancers.[21,22] In response to growth factor ligand binding, EGFR is significantly involved in cell signaling pathways associated with growth, differentiation and proliferation. Previous clinical trials involving EGFR-targeted therapies in cancer patients have shown promising increases in therapeutic efficacy and enhanced specificity.[23] Due to these reasons, we synthesize NDs which are endowed with the specificity of anti-EGFR monoclonal antibodies (mAbs), designed to increase internalization and delivery of anticancer agents into EGFR-overexpressing cells.

Paclitaxel (PTX), a chemotherapeutic which causes cell death by interrupting the polymerization dynamics of tubulin during cell division and interphase, remains as one of the most frequently used antitumor drugs against ovarian and breast cancer today.[24] Although highly effective, several challenges associated with drug administration remain, most notably side effects due to solubilization agents and drug resistance among others.[24,25] The commercial formulation of PTX, Taxol (Bristol-Myers Squibb), includes a 1:1 absolute ethanol:Cremophor EL solubilization agent, which has been associated with hypersensitivity reactions and many others.[24,26] Therefore, emerging nanoparticle-based delivery approaches for increasing PTX solubility and efficacy have been studied.[27–32] In this study, we report

Dr. X.-Q. Zhang,[+] Dr. H.-J. Kim, Prof. D. Ho
Department of Biomedical Engineering
Northwestern University Evanston
Illinois 60208, USA
E-mail: d-ho@northwestern.edu
R. Lam,[+] Prof. D. Ho
Department of Mechanical Engineering
Northwestern University Evanston
Illinois 60208, USA
Dr. X. Xu
Department of Chemistry
Northwestern University Evanston
Illinois 60208, USA
Dr. E. K. Chow
George Williams Hooper Foundation
University of California
San Francisco, San Francisco, CA 94143, USA
Prof. D. Ho
Institute for Bionanotechnology in Medicine (IBNAM)
Northwestern University Chicago
IL, 60611, USA
Prof. D. Ho
Robert H. Lurie Comprehensive Cancer Center
Chicago, IL 60611, USA
[+] X.-Q.Z. and R.L. contributed equally to this work.

DOI: 10.1002/adma.201102263

on a multimodal ND conjugate to improve the therapeutic index of PTX through targeting and nanoparticle attachment.

Within this construct, PTX molecules are attached to the ND surface via fluorescently labeled oligonucleotide strands. Polyvalent DNA functionalization of nanoparticles has been extensively studied and utilized in a variety of biological applications, including nanomedicine, diagnostics and self-assembly.[6,33–35] The programmable and versatile chemistry afforded by oligonucleotide synthesis is especially useful in drug delivery, as the simultaneous linkage and intracellular tracking of conjugated therapeutics to the ND surface can be accomplished in an integrated manner. DNA-functionalization has also been shown to exhibit a three orders of magnitude higher cellular uptake than oligoethylene glycol (OEG)-functionalized NPs, a commonly used linker.[6] Combined with anti-EGFR mAb attachment to the ND surface, the resultant conjugates provide a multimodal drug delivery platform with simultaneous capabilities in enhanced therapy, targeting and imaging. The collective capacity of this ND-based drug delivery system was then tested and observed in vitro within breast cancer cells of contrasting EGFR expression.

In order to prepare the multimodal ND nanoparticles possessing both fluorescently labeled drug-oligonucleotide conjugates and mAbs, the ND surface was first functionalized with the hetero-bifunctional cross-linker sulfosuccinimidyl 6-(3′-[2-pyridyldithio]propionamido)hexanoate (sulfo-LC-SPDP) and characterized with Fourier transform infrared spectroscopy (FTIR) (see Figure S1, Supporting Information), followed by the attachment of thiol-containing biomolecules (**Figure 1**a).

For PTX linkage, we first constructed a thiolated 20-mer poly-dT strand containing a terminal dodecyl amine for conjugation. A fluorescein-labeled dT-nucleotide was inserted within the oligonucleotide strand for cellular imaging and PTX loading quantification. A carboxylic acid derivative of PTX (Compound 1)[36] was tethered to the oligonucleotide strand via amine coupling chemistry (PTX-DNA) and characterized by matrix-assisted laser desorption/ionization mass spectrometry (MALDI-MS) (see Figure S2 and S3, Supporting Information). Sulfhydryl groups were introduced into the targeting protein by reacting 2-Iminothiolane (Traut's reagent) with primary amines within anti-EGFR mAbs (see Figure S4, Supporting Information). Resultant thiolated PTX-DNA and mAbs were then simultaneously coupled to SPDP functionalized NDs (ND-SPDP), forming PTX-DNA/mAb@NDs (Figure 1a).

Once functionalization was completed, conjugates were purified through repeated centrifugation and washes to remove excess unbound ligands, resulting in highly stable suspensions within aqueous solutions. Dynamic light scattering (DLS) analysis showed untargeted and targeted PTX-DNA@ND hydrodynamic sizes of ≈ 230 nm and ζ-potential values of ≈ −30 mV (Figure 1b,c).

A cleavable disulfide linkage between attached biological cargo (i.e. oligonucleotides, therapeutics and proteins) and the ND surface allows for the surface loading quantification of PTX

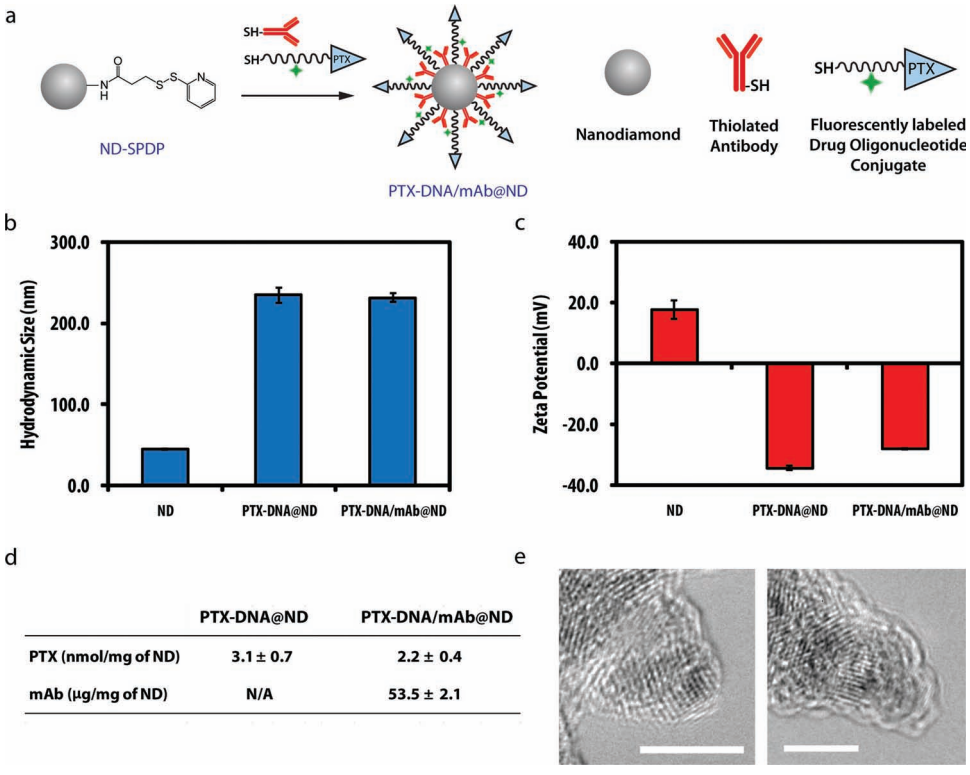

	PTX-DNA@ND	PTX-DNA/mAb@ND
PTX (nmol/mg of ND)	3.1 ± 0.7	2.2 ± 0.4
mAb (μg/mg of ND)	N/A	53.5 ± 2.1

Figure 1. a) Synthetic scheme of multifunctional PTX-DNA/mAb@NDs. Sulfo-LC-SPDP was attached on to an aminated ND surface (ND-NH_2), forming sulfhydryl-reactive NDs (ND-SPDPs). Thiolated drug-oligonucleotide conjugates and thiolated mAbs were then simultaneously attached to ND-SPDPs. b) Hydrodynamic size and c) ζ-potential of NDs and specified conjugates. Particles were suspended in deionized water (50 μg/ml) (N = 3). d) Surface loading of PTX and mAb within PTX-DNA@ND and PTX-DNA/mAb@ND conjugates. Data is represented as the mean ± standard deviation (N = 3). e) TEM images of (left) NDs and (right) PTX-DNA/mAb@NDs. Scale bars are 5 nm in each image.

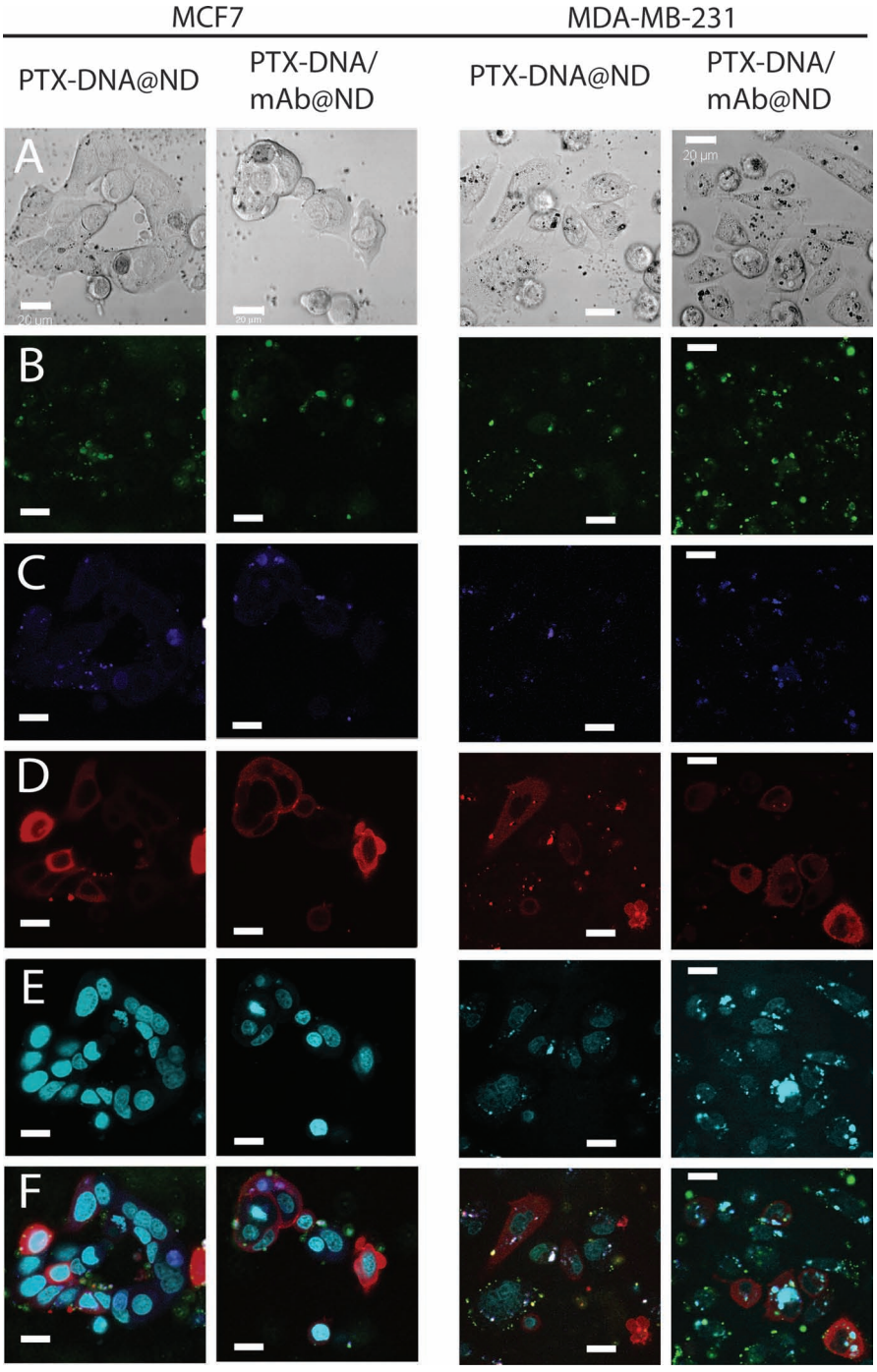

Figure 2. Confocal fluorescence microscopy images of live MCF7 and MDA-MB-231 cells treated with ND-conjugates (25 µg/ml) after 6 h. Each sample was imaged for a) bright field, b) oligonucleotide based fluorescein fluorescence, c) Lysotracker stained lysosomes, d) Cellular Lights stained actin, e) DRAQ5 stained nuclei and f) overlaid. Scale bars are 20 µm in each image.

and mAbs. Treatment with dithiothreitol (DTT) cleaves and detaches PTX-DNA and thiolated mAbs from the ND surface. Prior to DTT treatment, supernatant collection after centrifugation yielded a colorless liquid. In contrast, after DTT treatment, supernatant samples upon centrifugation produced a green fluorescent tint, indicating successful cleavage of fluorescently tagged PTX-DNA from the ND surface. Fluorescence analysis and protein quantification assays of collected supernatant revealed surface loading of 3.1 ± 0.7 nmol of PTX per mg of untargeted ND conjugates and 2.2 ± 0.4 nmol of PTX and 53.5 ± 2.1 µg of mAb per mg of targeted ND (Figure 1d). Transmission electron microscope (TEM) images also showed an amorphous organic layer coating the crystalline NDs within PTX-DNA/mAb@NDs as compared to ND only controls

(Figure 1e). These results clearly confirm the presence of PTX-DNA and mAb within PTX-DNA/mAb@ND conjugates and represent the versatility afforded by this delivery system.

The feasibility of PTX-DNA/mAb@NDs as a targeted drug delivery platform was tested through in vitro uptake studies in breast cancer models with upregulated EGFR as a readout within basal EGFR expressing MCF7 and EGFR-overexpressing MDA-MB-231 cells. By observing the fluorescent tag within the oligonucleotide linkers, the therapeutic payload delivery of the resultant conjugates can be examined through confocal microscopy. Internalization was measured within MDA-MB-231 cells compared with MCF7 cells. The differences in EGFR density allow for the comparison of baseline untargeted internalization within cells of normal level EGFR expression and increased uptake through targeted delivery in EGFR-overexpressing cells. Confocal microscopy data demonstrates that after 6 hours of incubation, PTX-DNA@ND and PTX-DNA/mAb@ND treated MCF7 cells exhibited similar levels of fluorescence (**Figure 2**). In contrast, anti-EGFR containing conjugates were highly fluorescent compared to the untargeted NDs within MDA-MB-231 cells (Figure 2, Channel B). These results attest to the internalization specificity conferred by anti-EGFR mAb during uptake. Fluorescence within all conjugates was primarily observed in the cytoplasm in a punctuate manner. Furthermore, a significant portion of conjugates were colocalized with lysosomes, consistent with observations from previous reports on an endocytic mechanism of internalization (Figure 2, Channel B and C).[37,38] These results suggest that the majority of complexes enter the endosomal pathway, but the addition of anti-EGFR improves the internalized amount in the same period of time.

Binding and uptake of EGFR-targeted and non-targeted NDs within EGFR-overexpressing cell lines were then quantitatively evaluated by flow cytometry (**Figure 3**). Fluorescence intensity of fluorescein-labeled DNA linkers within PTX-DNA@NDs and PTX-DNA/mAb@NDs showed that internalization was nearly equivalent within MCF7 cells, even in the presence of the soluble competitive binding agent EGF. However, when MDA-MB-231 cells were treated with PTX-DNA/mAb@NDs, there

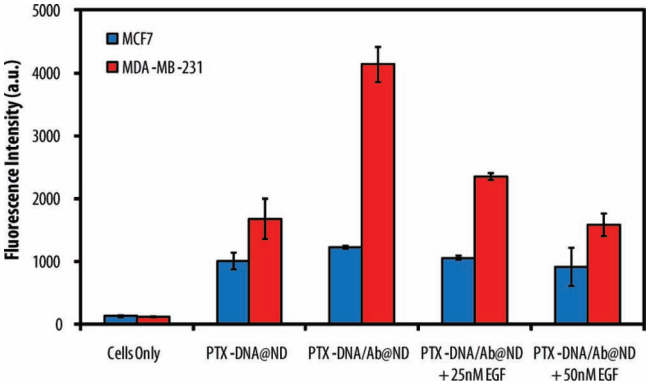

Figure 3. Quantitative analysis of PTX-DNA@ND and PTX-DNA/mAb@ND internalization within cells. Flow cytometry analysis of fluorescein-labeled oligonucleotides is representative of ND-conjugate internalization into MCF7 and MDA-MB-231 cells. Data is represented as the mean ± standard deviation (N = 2).

was a nearly 150% enhancement in the fluorescence signal as compared to that of PTX-DNA@NDs. Internalization of anti-EGFR-conjugated NDs within MDA-MB-231 cells was competitively inhibited by the addition of soluble EGF. Increased concentrations of EGF led to larger reductions of internalization. At excess amounts of EGF, internalization was reduced to original base level internalization found in untargeted PTX-DNA@NDs. Therefore, results show the large enhancement in delivery within EGFR-overexpressing cells is primarily attributed to the specific targeting conferred by mAb conjugation.

We then investigated the effect of targeted delivery of the ND conjugates towards enhancing cellular cytotoxicity. MTT viability assays were first assessed for ND-only controls (see Figure S5, Supporting Information). Cell viability was >90% for ND concentrations up to 200 μg/ml, attesting to NDs as a biocompatible nanocarrier. The same assays were then performed comparing free PTX with untargeted and targeted versions of PTX-DNA@NDs at equivalent PTX dosages in MCF7 and MDA-MB-231 cells (**Figure 4**). Enhanced cytotoxicity was observed in escalating-dose

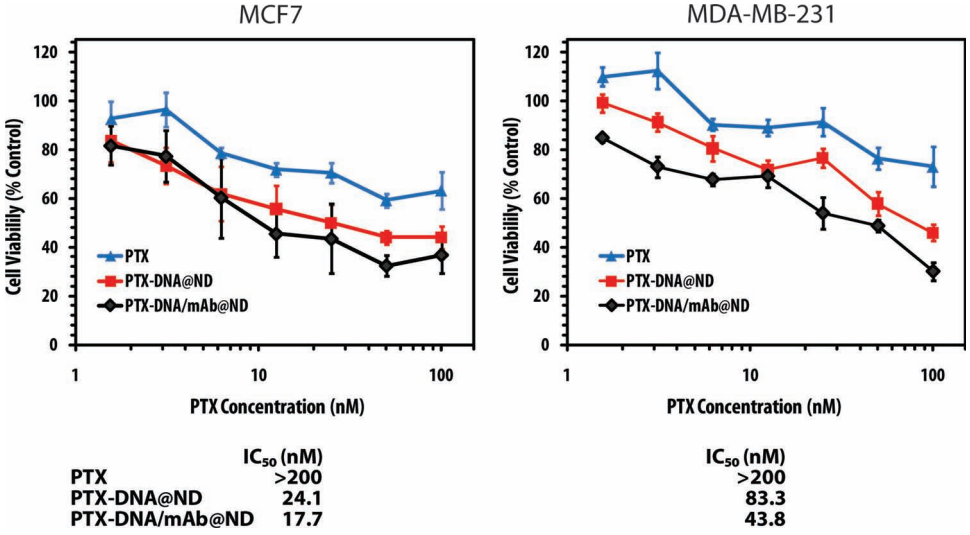

Figure 4. Cytotoxicity profiles of PTX (blue triangles), PTX-DNA@NDs (red squares) and PTX-DNA/mAb@NDs (black diamonds) in respect to escalating equivalent PTX doses in MCF7 and MDA-MB-231 cells after 48 h incubation ($n = 6$). Corresponding IC_{50} values are listed underneath.

studies after 48 h treatment of PTX-DNA@NDs and PTX-DNA/mAb@NDs in both cell lines across all concentrations. Since only ~32 and ~45 μg/ml of NDs were employed within 100 nM PTX dosages in untargeted and targeted conjugates, respectively, the reduction in viability can be solely attributed to PTX activity. In MCF7 and MDA-MB-231 cells, PTX performed with similar efficiency with IC_{50} values of over 200 nM. Untargeted and targeted PTX-DNA@NDs in MCF7 cells, possessed IC_{50} values of 24.1 nM and 17.7 nM, respectively. These results attest to the enhanced activity of PTX when tethered to the ND surface, similar to previously reported results.[28,33] However, targeted conjugates did not show a significant improvement in cytotoxicity compared to untargeted PTX-DNA@NDs, presumably due to the negligible effect of targeting towards normal EGFR expression. In contrast, anti-EGFR linked conjugates had an IC_{50} value of 43.8 nM within MDA-MB-231 cells, a nearly two-fold increase in efficacy compared to untargeted conjugates. The data suggests that targeting through the mAb moiety increases specificity and internalization, which subsequently enhances therapeutic activity. As such, increased EGFR density on the plasma membrane amplifies delivery and the ability to mediate selectivity cytotoxicity.

In conclusion, heterofunctional NDs were prepared by attaching fluorescently labeled PTX-DNA conjugates and anti-EGFR mAbs onto the ND surface, alluding to the utility of targeted NDs as a novel drug-delivery platform for applications in oncology. The covalent attachment of PTX and mAbs significantly enhanced therapeutic activity and targeting specificity. Fluorescently labeled oligonucleotide linkers within conjugates enabled intracellular observation and uptake measurements through confocal microscopy and flow cytometry, respectively. Visualization of fluorescein-labeled targeted and untargeted PTX-DNA@ND conjugates revealed internalization and targeting profiles within cells of disparate EGFR expression. MAb linked conjugates were found to have very little effect within MCF7 cells due to basal EGFR expression. In contrast, PTX-DNA/mAb@NDs efficiently internalized into EGFR-overexpressing MDA-MB-231 cells through multivalent interactions, exhibiting significantly enhanced uptake and therapeutic efficacy. To demonstrate the over-expression of EGFR in MDA-MB-231 cells, the elevated uptake of targeted conjugates was suppressed in the presence of a competitive binding factor, EGF. IC_{50} values indicated that drug conjugation onto the ND surface demonstrated an order of magnitude greater potency than free drug within MCF7 breast cancer cell lines. Notably, the addition of anti-EGFR mAbs as an active targeting ligand resulted in a further two-fold increase in therapeutic activity over untargeted drug-ND conjugates in MDA-MB-231 EGFR-overexpressing tumor cells. The next phase of our studies will involve evaluating the in vivo efficacy of the targeted ND drug conjugates in animal models of cancer. Finally, these versatile heterofunctionalized ND conjugates provide an excellent platform for developing next-generation targeted nanomedicine strategies.

Experimental Section

For experimental details see supporting information.

Supporting Information

Supporting Information is available from the Wiley Online Library or from the author.

Acknowledgements

The authors acknowledge the Chad Mirkin research group for their fruitful discussions. The authors acknowledge the use of the characterization facilities at the Electron Probe Instrumentation Center (EPIC), Keck Interdisciplinary Surface Science (Keck-II) Center and Integrated Molecular Structure Education and Research Center (IMSERC) at Northwestern University. Flow cytometry work was performed at the Robert H. Lurie Comprehensive Cancer Center Flow Cytometry Core (RHLCCC) Facility and supported by the Northwestern University Flow Cytometry Facility and Cancer Center Support Grant (NCI CA060553). Imaging work was performed at the Northwestern University Cell Imaging Facility generously supported by NCI CCSG P30 CA060553 awarded to the Robert H Lurie Comprehensive Cancer Center. D.H. was supported by the National Science Foundation CAREER Award (CMMI-0846323), Mechanics of Materials grant CMMI-0856492, Center for Scalable and Integrated NanoManufacturing (DMI-0327077), National Center for Learning & Teaching, V Foundation for Cancer Research Scholars Award, and Wallace H. Coulter Foundation Translational Research Award, as well as the European Commission funding program FP7-KBBE-2009-3. R.L. acknowledges the Northwestern Ryan Fellowship.

Received: June 16, 2011
Revised: August 12, 2011
Published online: September 20, 2011

[1] D. Peer, J. M. Karp, S. Hong, O. C. Farokhzad, R. Margalit, R. Langer, *Nat. Nanotechnol.* **2007**, *2*, 751.
[2] P. Alivisatos, *Nat. Biotechnol.* **2004**, *22*, 47.
[3] Y. Jin, C. Jia, S.-W. Huang, M. O'Donnell, X. Gao, *Nat. Commun.* **2010**, *1*, 41.
[4] A. S. Paraskar, S. Soni, K. T. Chin, P. Chaudhuri, K. W. Muto, J. Berkowitz, M. W. Handlogten, N. J. Alves, B. Bilgicer, D. M. Dinulescu, R. A. Mashelkar, S. Sengupta, *Proc. Natl. Acad. Sci. USA* **2010**, *107*, 12435.
[5] M. E. Davis, J. E. Zuckerman, C. H. J. Choi, D. Seligson, A. Tolcher, C. A. Alabi, Y. Yen, J. D. Heidel, A. Ribas, *Nature* **2010**, *464*, 1067.
[6] D. A. Giljohann, D. S. Seferos, W. L. Daniel, M. D. Massich, P. C. Patel, C. A. Mirkin, *Angew. Chem. Int. Ed.* **2010**, *49*, 3280.
[7] Z. Liu, S. M. Tabakman, Z. Chen, H. Dai, *Nat. Protoc.* **2009**, *4*, 1372.
[8] A. M. Schrand, H. Huang, C. Carlson, J. J. Schlager, E. Osawa, S. M. Hussain, L. Dai, *J. Phys. Chem. B* **2007**, *111*, 2.
[9] H. Huang, E. Pierstorff, E. Osawa, D. Ho, *Nano Lett.* **2007** *7*, 3305
[10] S. Vial, C. Mansuy, S. Saga, T. Irinopoulo, F. Burlina, J.-P. Boudou, G. Chassaing, S. Lavielle, *ChemBioChem* **2008**, *9*, 2113.
[11] A. Krueger, *Chem.-Eur. J.* **2008**, *14*, 1382.
[12] A. S. Barnard, *J. Mater. Chem.* **2008**, *18*, 4038.
[13] E. K. Chow, X.-Q. Zhang, M. Chen, R. Lam, E. Robinson, H. Huang, D. Schaffer, E. Osawa, A. Goga, D. Ho, *Sci. Transl. Med.* **2011**, *3*, 73ra21. *DOI:* 10.1126/scitranslmed.3001713
[14] S. J. Yu, M. W. Kang, H. C. Chang, K. M. Chen, Y. C. Yu, *J. Am. Chem. Soc.* **2005**, *127*, 17604.
[15] F. Neugart, A. Zappe, F. Jelezko, C. Tietz, J. P. Boudou, A. Krueger, J. Wrachtrup, *Nano Lett.* **2007**, *7*, 3588.
[16] C.-C. Fu, H.-Y. Lee, K. Chen, T.-S. Lim, H.-Y. Wu, P.-K. Lin, P.-K. Wei, P.-H. Tsao, H.-C. Chang, W. Fann, *Proc. Natl. Acad. Sci. USA* **2007**, *104*, 727.
[17] X.-Q. Zhang, M. Chen, R. Lam, X. Xu, E. Osawa, D. Ho, *ACS Nano* **2009**, *3*, 2609.

[18] C. Bradac, T. Gaebel, N. Naidoo, M. J. Sellars, J. Twamley, L. J. Brown, A. S. Barnard, T. Plakhotnik, A. V. Zvyagin, J. R. Rabeau, *Nat. Nanotechnol.* **2010**, *5*, 345.
[19] Y. R. Chang, H. Y. Lee, K. Chen, C. C. Chang, D. S. Tsai, C. C. Fu, T. S. Lim, Y. K. Tzeng, C. Y. Fang, C. C. Han, H. C. Chang, W. Fann, *Nat. Nanotechnol.* **2008**, *3*, 284.
[20] O. C. Farokhzad, R. Langer, *ACS Nano* **2009**, *3*, 16.
[21] J. D. Byrne, T. Betancourt, L. Brannon-Peppas, *Adv. Drug Delivery Rev.* **2008**, *60*, 1615.
[22] J. J. Laskin, A. B. Sandler, *Cancer Treat. Rev.* **2004**, *30*, 1.
[23] C. M. Rocha-Lima, H. P. Soares, L. E. Raez, R. Singal, *Cancer Control* **2007**, *14*, 295.
[24] A. K. Singla, A. Garg, D. Aggarwal, *Int. J. Pharm.* **2002**, *235*, 179.
[25] R. Panchagnula, *Int. J. Pharm.* **1998**, *172*, 1.
[26] R. T. Dorr, *Ann. Pharmacother.* **1994**, *28*, S11.
[27] J. R. Hwu, Y. S. Lin, T. Josephrajan, M.-H. Hsu, F.-Y. Cheng, C.-S. Yeh, W.-C. Su, D.-B. Shieh, *J. Am. Chem. Soc.***2008**, *131*, 66.
[28] Z. Liu, K. Chen, C. Davis, S. Sherlock, Q. Cao, X. Chen, H. Dai, *Cancer Res.* **2008**, *68*, 6652.
[29] Y. Zhang, L. Tang, L. Sun, J. Bao, C. Song, L. Huang, K. Liu, Y. Tian, G. Tian, Z. Li, H. Sun, L. Mei, *Acta Biomater.* **2010**, *6*, 2045.
[30] A. P. Griset, J. Walpole, R. Liu, A. Gaffey, Y. L. Colson, M. W. Grinstaff, *J. Am. Chem. Soc.* **2009**, *131*, 2469.
[31] V. P. Torchilin, A. N. Lukyanov, Z. Gao, B. Papahadjopoulos-Sternberg, *Proc. Natl. Acad. Sci. USA* **2003**, *100*, 6039.
[32] J. D. Gibson, B. P. Khanal, E. R. Zubarev, *J. Am. Chem. Soc.* **2007**, *129*, 11653.
[33] S. Dhar, W. L. Daniel, D. A. Giljohann, C. A. Mirkin, S. J. Lippard, *J. Am. Chem. Soc.* **2009**, *131*, 14652.
[34] C. A. Mirkin, R. L. Letsinger, R. C. Mucic, J. J. Storhoff, *Nature* **1996**, *382*, 607.
[35] R. Elghanian, J. J. Storhoff, R. C. Mucic, R. L. Letsinger, C. A. Mirkin, *Science* **1997**, *277*, 1078.
[36] H. M. Deutsch, J. A. Glinski, M. Hernandez, R. D. Haugwitz, V. L. Narayanan, M. Suffness, L. H. Zalkow, *J. Med. Chem.* **1989**, *32*, 788.
[37] K.-K. Liu, C.-C. Wang, C.-L. Cheng, J.-I. Chao, *Biomaterials* **2009**, *30*, 4249.
[38] O. Faklaris, V. Joshi, T. Irinopoulou, P. Tauc, M. Sennour, H. Girard, C. l. Gesset, J.-C. Arnault, A. Thorel, J.-P. Boudou, P. A. Curmi, F. o. Treussart, *ACS Nano* **2009**, *3*, 3955.